JOC Article
pubs.acs.org/joc

Supramolecular Complexation and Enantiodifferentiating Photocyclodimerization of 2-Anthracenecarboxylic Acid with 4-Aminoprolinol Derivatives as Chiral Hydrogen-Bonding Templates

Yuko Kawanami,[†] Tamara C. S. Pace,[‡] Jun-ichi Mizoguchi,[§] Toshiharu Yanagi,[§] Masaki Nishijima,[†] Tadashi Mori,[†] Takehiko Wada,[†,∥] Cornelia Bohne,*[,‡] and Yoshihisa Inoue*[,†]

[†]*Department of Applied Chemistry and Center for Advanced Science and Innovation, Osaka University, 2-1 Yamadaoka, Suita 565-0871, Japan,* [‡]*Department of Chemistry, University of Victoria, P.O. Box 3065, Victoria, BC, Canada V8W 3V6, and* [§]*Bio/Fine Chemicals Department, Nagase ChemteX Corporation, 2-2-3 Murotani, Nishi-ku, Kobe 651-2241, Japan.* [∥]*Present address: Institute of Multidisciplinary Research for Advanced Materials, Tohoku University, 2-1-1 Katahira, Aoba, Sendai 980-8577, Japan*

bohne@uvic.ca; inoue@chem.eng.osaka-u.ac.jp

Received August 18, 2009

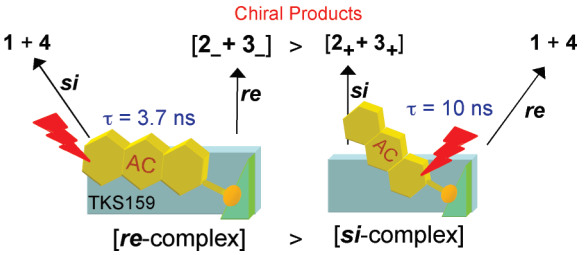

The photochirogenesis of 2-anthracenecarboxylic acid (AC) complexed to a hydrogen-bonding template (TKS159) was investigated to obtain mechanistic information on how chirogenesis is achieved for the dimerization of AC. Complexation of AC to TKS159 leads to the shielding of one of the two surfaces of the prochiral AC molecule. The two diastereomeric AC−TKS complexes, i.e., *re*-AC−TKS and *si*-AC−TKS, were characterized by changes in the UV−vis, fluorescence, and circular dichroism spectra and excited-state lifetimes. The ee is not simply determined by the diastereomeric ratio of the *re*- and *si*-AC−TKS complexes but also depends on the relative lifetimes of the diastereomeric complexes. The relative population of the *re* and *si* complexes was calculated from the enantiomeric excess (ee) for the products, taking into account the relative lifetimes of the two complexes. These studies established a protocol that can be used to reveal the mechanism for photochirogenesis by investigating the ground state and the excited state behavior of supramolecular systems.

Introduction

Chirality is prevalent in nature and is essential in many biological functions. In this context, supramolecular photochirogenesis is one approach being developed to understand how chirogenesis can be achieved and manipulated.[1−5] A chiral environment is required when prochiral reactants are used, and this chiral environment can be achieved in anisotropic media, such as solids[6−12] or

(1) Griesbeck, A. G.; Meierhenrich, U. J. *Angew. Chem.* **2002**, *41*, 3147–3154.
(2) Inoue, Y. *Chem. Rev.* **1992**, *92*, 741–770.
(3) Müller, C.; Bach, T. *Aust. J. Chem.* **2008**, *61*, 557–564.
(4) Wada, T.; Inoue, Y. In *Chiral Photochemistry*; Inoue, Y., Ramamurthy, V., Eds.; Marcel Dekker: New York, 2004; pp 341−384.
(5) Yang, C.; Inoue, Y. In *Cyclodextrin Materials Photochemistry, Photophysics and Photobiology*; Douhal, A., Ed.; Elsevier: New York, 2006; pp 241−265.
(6) Chong, K. C. W.; Sivaguru, J.; Schichi, T.; Yoshimi, Y.; Ramamurthy, V.; Scheffer, J. R. *J. Am. Chem. Soc.* **2002**, *124*, 2858–2859.
(7) Joy, A.; Ramamurthy, V.; Scheffer, J. R.; Corbin, D. R. *Chem. Commun.* **1998**, 1379–1380.
(8) Joy, A.; Scheffer, J. R.; Ramamurthy, V. *Org. Lett.* **2000**, *2*, 119–121.
(9) Scheffer, J. R. In *Chiral Photochemistry*; Inoue, Y., Ramamurthy, V., Eds.; Marcel Dekker: New York, 2004.
(10) Braga, D.; Grepioni, F. *Angew. Chem.* **2004**, *43*, 4002–4011.
(11) Matsumoto, A. *Top. Curr. Chem.* **2005**, *254*, 263–305.
(12) Tanaka, K.; Toda, F. *Chem. Rev.* **2000**, *100*, 1025–1074.

Published on Web 09/17/2009 DOI: 10.1021/jo901792t

SCHEME 1. Photocyclodimerization of 2-Anthracenecarboxylic Acid (AC) and Chiral Templates TKS159 and TM166 That Are Epimeric to Each Other

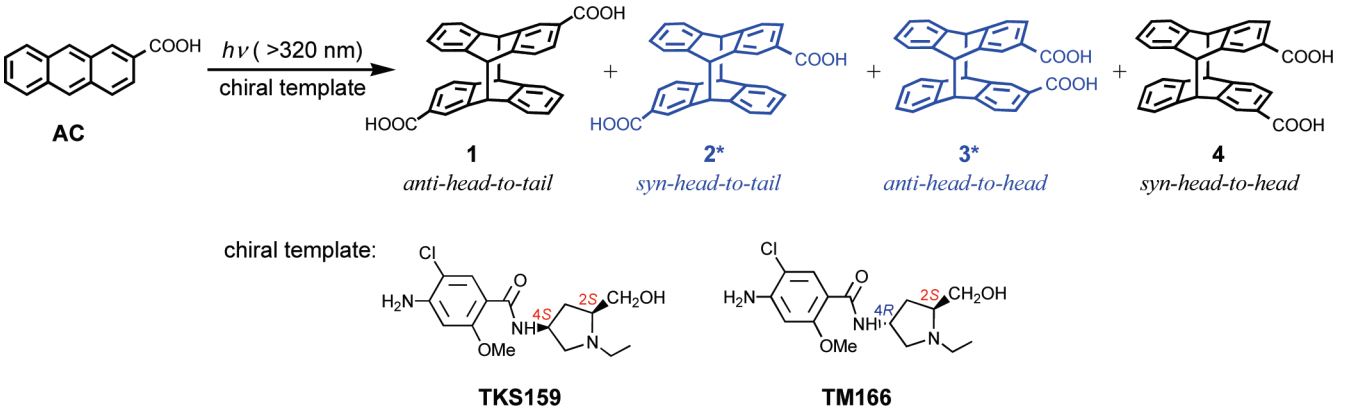

liquid crystals[13,14] or in isotropic media with the use of chiral host systems.[4] Examples of supramolecular host systems in solution for which photochirogenesis has been investigated include cyclodextrins,[15−21] DNA,[22] and hydrogen-bonding templates.[23−25]

In anisotropic solid media the spatial relationship is well-defined and dictates the stereochemical outcome of reactions. Mechanistic information is drawn from the knowledge of the spatial distribution of molecules in the media, but changes in the stereochemical outcome are frequently difficult to achieve without changing the whole medium. In contrast, supramolecular host−guest systems in isotropic media provide the ability to manipulate the conformations and orientations of the prochiral reactants in the chiral host systems by making subtle changes in environmental factors within the host−guest system without having to change the bulk environment, i.e., the solvent system. The drawback for the use of supramolecular systems in isotropic media is that mechanistic information is not as readily available as that from the structural determination in anisotropic media. Therefore, it is essential to develop experimental approaches to elucidate the mechanisms that operate in photochirogenesis in isotropic media to establish the conceptual framework necessary for the design of new chiral hosts with increased chiral discrimination ability.

Photochirogenesis has been achieved previously with the use of hydrogen-bonding templates, such as templates based on the amide functionality.[23,24,26−34] Host−guest binding was directed by a small number (two or three) of hydrogen bonds, and stereochemical control was accomplished for photochemical reactions by shielding one of the enantiofaces of the prochiral molecule. Moderate to high enantiomeric excesses (ee) were observed. Many of the reactions studied were unimolecular, but examples were also reported for bimolecular reactions where one reaction partner is complexed to the chiral template.[35,36]

Photochirogenesis involving bimolecular reactions adds another layer of complexity because the two reaction partners can either be in close proximity at the time of excitation or they have to diffuse and form an encounter complex before products are formed. Anthracenes photodimerize readily,[37,38] and when asymmetrically substituted, such as in the case of 2-anthracenecarboxylic acid (AC), form four configurational isomers of which two products are chiral (Scheme 1). The photodimerization of AC has been used as a model reaction in several supramolecular systems.[17,18,20,21,39−43]

(13) Leigh, W. J.; Workentin, M. S. In *Handbook of Liquid Crystals*; Demun, D., Ed.; Wiley-VCH: Weinheim, 1998; pp 839−895.
(14) Ishida, Y.; Kai, Y.; Kato, S.; Misawa, A.; Mano, S.; Matsuoka, Y.; Saigo, K. *Angew. Chem.* **2008**, *47*, 8241–8245.
(15) Inoue, Y.; Dong, F.; Yamamoto, K.; Tong, L.-H.; Tsuneishi, H.; Hakushi, T.; Tai, A. *J. Am. Chem. Soc.* **1995**, *117*, 11033–11034.
(16) Inoue, Y.; Wada, T.; Sugahara, N.; Yamamoto, K.; Kimura, K.; Tong, L.; Gao, X.; Hou, Z.; Liu, Y. *J. Org. Chem.* **2000**, *65*, 8041–8050.
(17) Nakamura, A.; Inoue, Y. *J. Am. Chem. Soc.* **2003**, *125*, 966–972.
(18) Nakamura, A.; Inoue, Y. *J. Am. Chem. Soc.* **2005**, *127*, 5338–5339.
(19) Rao, V. P.; Turro, N. J. *Tetrahedron Lett.* **1989**, *30*, 4641–4644.
(20) Tamaki, T.; Kokubu, T.; Ichimura, K. *Tetrahedron* **1987**, *43*, 1485–1494.
(21) Yang, C.; Nakamura, A.; Fukuhara, G.; Origane, Y.; Mori, T.; Wada, T.; Inoue, Y. *J. Org. Chem.* **2006**, *71*, 3126–3136.
(22) Wada, T.; Sugahara, N.; Kawano, M.; Inoue, Y. *Chem. Lett.* **2000**, 1174–1175.
(23) Bach, T.; Bergmann, H.; Grosch, B.; Harms, K. *J. Am. Chem. Soc.* **2002**, *124*, 7982–7990.
(24) Cauble, D. F.; Lynch, V.; Krische, M. J. *J. Org. Chem.* **2003**, *68*, 15–21.
(25) Mizoguchi, J.; Kawanami, Y.; Wada, T.; Kodama, K.; Anzai, K.; Yanagi, T.; Inoue, Y. *Org. Lett.* **2006**, *8*, 6051–6054.
(26) Aechtner, T.; Dressel, M.; Bach, T. *Angew. Chem.* **2004**, *43*, 5849–5851.
(27) Bach, T.; Aechtner, T.; Neumülller, B. *Chem. Eur. J.* **2002**, *8*, 2464–2475.
(28) Bach, T.; Bergmann, H. *J. Am. Chem. Soc.* **2000**, *122*, 11525–11526.
(29) Bach, T.; Bergmann, H.; Harms, K. *Angew. Chem.* **2000**, *39*, 2302–2304.
(30) Bach, T.; Bergmann, H.; Harms, K. *Org. Lett.* **2001**, *3*, 601–603.
(31) Bauer, A.; Westkämper, F.; Grimme, S.; Bach, T. *Nature* **2005**, *436*, 1139–1140.
(32) Brandes, S.; Seiling, P.; Bach, T. *Synlett* **2004**, *14*, 2588–2590.
(33) Selig, P.; Bach, T. *J. Org. Chem.* **2006**, *71*, 5662–5673.
(34) Müller, C.; Bauer, A.; Bach, T. *Angew. Chem.* **2009**, *48*.
(35) Grosch, B.; Orlebar, C. N.; Herdtwec, E.; Kaneda, M.; Wada, T.; Inoue, Y.; Bach, T. *Chem. Eur. J.* **2004**, *10*, 2179–2189.
(36) Grosch, B.; Orlebar, C. N.; Herdtweck, E.; Massa, W.; Bach, T. *Angew. Chem.* **2003**, *42*, 3693–3696.
(37) Bouas-Laurent, H.; Castellan, A.; Desvergne, J.-P.; Lapouyade, R. *Chem. Soc. Rev.* **2000**, *29*, 43–55.
(38) Bouas-Laurent, H.; Castellan, A.; Desvergne, J.-P.; Lapouyade, R. *Chem. Soc. Rev.* **2001**, *30*, 248–263.
(39) Yang, C.; Fukuhara, G.; Nakamura, A.; Origane, Y.; Fujita, K.; Yuan, D.-Q.; Mori, T.; Wada, T.; Inoue, Y. *J. Photochem. Photobiol., A* **2005**, *173*, 375–383.
(40) Yang, C.; Nakamura, A.; Wada, T.; Inoue, Y. *Org. Lett.* **2006**, *8*, 3005–3008.
(41) Wada, T.; Nishijima, M.; Fujisawa, T.; Sugahara, N.; Mori, T.; Nakamura, A.; Inoue, Y. *J. Am. Chem. Soc.* **2003**, *125*, 7492–7493.
(42) Nishijima, M.; Pace, T. C. S.; Nakamura, A.; Mori, T.; Wada, T.; Bohne, C.; Inoue, Y. *J. Org. Chem.* **2007**, *72*, 2707–2715.
(43) Nishijima, M.; Wada, T.; Mori, T.; Pace, T. C. S.; Bohne, C.; Inoue, Y. *J. Am. Chem. Soc.* **2007**, *129*, 3478–3479.

The formation of **3** with an ee of 70−80% was observed when the photodimerization was performed in a smectic liquid crystal formed using a chiral mesogen. A very low ee (2%) was observed when 1-anthracenecarboxylate was incorporated in this liquid crystal.[14] A similar strategy using a chiral cationic gelator has also been applied for the photodimerization of AC incorporated as counteranion in the gel to give exclusively the head-to-head cyclodimers but only −10% ee for **3**.[44] It is important to note that these examples constitute a reaction in a "rigid chiral" anisotropic environment. AC photodimerization was studied when two AC molecules form complexes with γ-cyclodextrin (γ-CD).[17,18,20,21,39,40] This reaction occurs immediately upon excitation because the two reaction partners are incorporated in the same γ-CD cavity. The ee for **2** and **3** for the native γ-CD were +32% and −3%, respectively, where the "+" and "−" signs are related to the order of elution from the HPLC column and are not assigned to an absolute configuration.[17] The ee for **2** was changed to −58% when a capped γ-CD was employed,[40] while the ee for **3** can be changed to −41% using electrostatic interactions in a γ-CD modified with a pendant arm containing positive charges.[18] These examples show how changes to a chiral host system in solution lead to significant changes in the ee for the chiral products of a bimolecular photoreaction. The photodimerization of AC in bovine[41,42] and human serum albumin[43,45] is one example where the chirogenesis is the outcome of a dynamic reaction. The proteins have several binding sites for AC and in the case of bovine serum albumin the highest ee was observed for AC bound to a site with modest binding affinity. In the case of human serum albumin a very high ee was observed (79% for **2** and 88% for **3**) at moderate AC/protein ratios (3−5), while a modest ee (50% for **2** and 14% for **3**) persisted even when most of the AC was bound to weak binding sites of the protein. The presence of multiple binding sites on the protein makes it difficult to unravel the mechanistic aspects that influence the enhancement of photochirogenesis in a dynamic bimolecular reaction.

AC is a prochiral molecule, where reactivity on each face leads to different isomers and in the case of products **2** and **3** to different enantiomers. A different way to study how chirogenesis is achieved in the bimolecular dynamic reaction between two ACs is to impede the access of the second AC molecule to one of the prochiral faces of the AC excited state. Preliminary experiments using (2*S*,4*S*)-4-amino-5-chloro-2-methoxy-*N*-(1-ethyl-2-hydroxymethyl-4-pyrrolidinyl)benzamide (TKS159,[46,47] Scheme 1) or its enantiomer as templates showed that the ee values for both **2** and **3** were enhanced.[25] NMR analysis of the AC−TKS complex showed that TKS159 shielded one face of the aromatic moiety of AC.[25] This templating approach is akin to the template strategy pioneered by Bach to induce photochirogenesis for unimolecular and bimolecular reactions.[23,26−36]

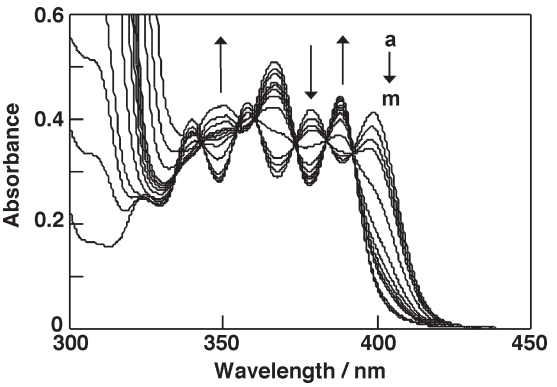

FIGURE 1. UV/vis absorption spectra of 0.1 mM AC in CH_2Cl_2 upon gradual addition of TKS159 at 25 °C. TKS/AC ratios: (a) 0, (b) 0.2, (c) 0.4, (d) 0.6, (e) 1.6, (f) 3.6, (g) 5.6, (h) 7.6, (i) 9.6, (j) 11.6, (k) 30, (l) 60, and (m) 120.

The host−guest complex involving the chiral template and prochiral reactant provide a chiral environment for the reaction to occur, while the lability of the supramolecular system is instrumental for the release of the product. These features are essential[48] to achieve the catalytic photochirogenesis observed by Bach and co-workers.[31,34]

The objective of the present work was to obtain mechanistic information on how photochirogenesis occurs by combining information from studies on the characterization of the AC−TKS complex, product distribution, and the photophysics of AC. Studies at different TKS/AC ratios and temperatures were required to find conditions where the reactivity of free AC was minimized and the formation of AC hydrogen-bonded dimers, present at low temperatures, was absent. Complexation of AC to TKS159 led to the formation of two diastereomeric complexes for which different lifetimes are observed for the singlet excited state of AC. This observation is the first experimental proof for the involvement of two diastereomeric precursor complexes in the photochirogeneses with chiral supramolecular hosts including chirally modified zeolites, cyclodextrins, hydrogen-bonding templates, chiral liquid crystals, chiral gels, and serum albumins. Furthermore, we have unequivocally demonstrated that in supramolecular photochirogenesis the enantioselectivities are not determined simply by the population of the diastereomeric precursor complexes in the ground state but are also affected significantly by their excited-state lifetimes. This established a standard protocol to fully elucidate the photophysics and photochemistry of supramolecular photochirogenesis and developed a few approaches to control/enhance the product's enantioselectivity, which will be applicable to many other supramolecular photochirogenic systems and make significant contribution to this rapidly developing interdisciplinary area of photochemistry and supramolecular chemistry.

Results

Characterization of the AC−TKS and AC−TM Complexes. The binding of AC as a guest to host systems, such as cyclodextrins[17,21,40] and serum albumins,[41−43,45] led to changes in the AC absorption, circular dichroism (CD), and

(44) Dawn, A.; Fujita, N.; Haraguchi, S.; Sada, K.; Shinkai, S. *Chem. Commun.* **2009**, 2100–2102.
(45) Pace, T. C. S.; Nishijima, M.; Wada, T.; Inoue, Y.; Bohne, C. *J. Phys. Chem. B* **2009**, *113*, 10445–10453.
(46) Matsuyama, S.; Sakiyama, H.; Nei, K.; Tanaka, C. *J. Pharmacol. Exp. Ther.* **1996**, *276*, 989–995.
(47) Yanagi, T.; Kitajima, A.; Anzai, K.; Kodama, K.; Mizoguchi, J.; Fujiwara, H.; Sakiyama, H.; Kamoda, O.; Kamei, C. *Chem. Pharm. Bull.* **1999**, *47*, 1650–1654.
(48) Inoue, Y. *Nature* **2005**, *436*, 1099–1100.

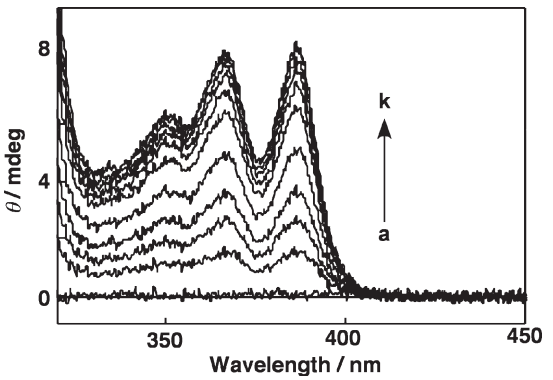

FIGURE 2. Induced CD spectra of 0.1 mM AC in CH_2Cl_2 at various concentrations of TKS159 at 10 °C. TKS/AC ratios: (a) 0, (b) 0.4, (c) 0.8, (d) 1.2, (e) 2.0, (f) 3.6, (g) 5.2, (h) 7.6, (i) 10.8, (j) 14.0, and (k) 19.6.

fluorescence spectra. These changes are associated with the formation of complexes and can be used to determine complex stability constants (K) and stoichiometries. The addition of TKS159 (Figure 1) and TM166 (Figure S1 in the Supporting Information) to AC solutions led to a blue shift in the AC absorption. TKS does not absorb above 350 nm (Figure S2 in the Supporting Information), and therefore, the changes observed above 350 nm are due to the incorporation of AC in an environment different from the homogeneous solvent, dichloromethane. Inspection of the absorbance values at the wavelengths close to the crossing points in the spectra showed some variability, which changed somewhat between independent experiments. This experimental variability makes it difficult to determine if isosbestic points are present for all TKS/AC ratios. The same trends for the changes in the AC absorption spectra with the addition of TKS were observed at lower temperatures.

AC when added to dichloromethane is in its protonated form. Addition of triethylamine to AC in dichloromethane led to a blue shift of the AC absorption spectrum (Figure S3 in the Supporting Information), which is more pronounced than the blue shift observed when AC is bound to TKS. This result suggests that binding of AC to TKS led to a partial deprotonation of AC and shows that hydrogen bonding plays a role in the complex formation.

AC is an achiral molecule and for this reason does not show an intrinsic circular dichroism (CD) signal. In the presence of TKS159 (Figure 2), but not TM166 (Figure S4 in the Supporting Information), an induced CD spectrum was observed in the spectral region where AC absorbs. This result indicates that AC is located in a chiral environment when bound to TKS159. In contrast, binding of AC to TM166 does not lead to a chiral environment around AC. This result is in agreement with the crystal structure determined for the AC−TM complex, where AC is hydrogen bonded to TM166 forming an extended complex.[25] In this complex, the AC and TM166 chromophores are not in close contact. The CD spectra could not be measured below 320 nm because the absorption of TKS159 is too strong at wavelengths shorter than 320 nm (see Figure S2 in the Supporting Information).

The fluorescence of AC decreased with the addition of TKS159 and TM166 (see Figure S5 in the Supporting Information). This decrease suggests that the emission efficiency for AC bound to TKS159 and TM166 is lower than that

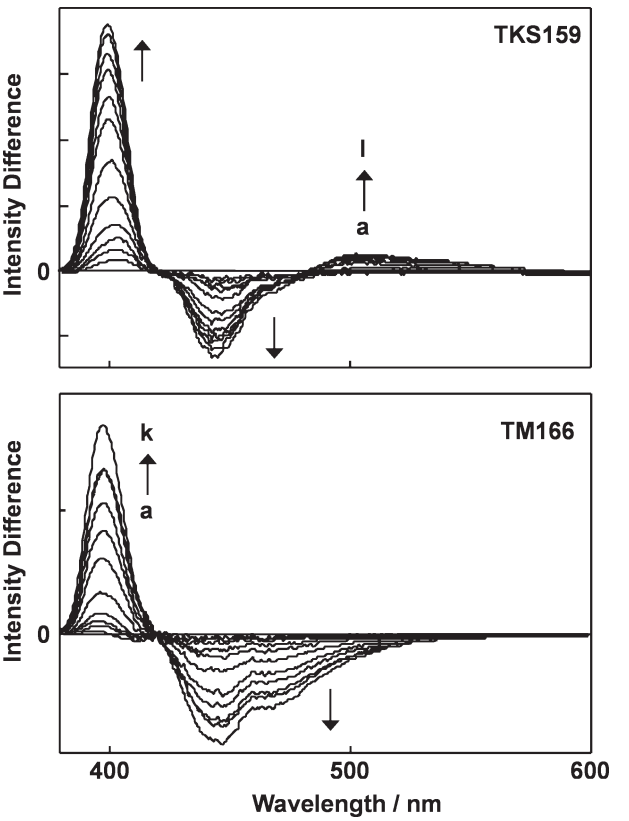

FIGURE 3. Difference spectra at 25 °C of the fluorescence spectra normalized at 420 nm for AC (0.025 mM) in the presence of varying amounts of TKS159 and the spectrum in the absence of TKS159 (top, TKS/AC ratios: (a) 0.54, (b) 1.2, (c) 1.6, (d) 2.7, (e) 5.3, (f) 10.7, (g) 18.7, (h) 26.7, (i) 40.0, (j) 53.3, (k) 80, and (l) 107). TM166 (bottom, TM/AC ratios: (a) 0.54, (b) 1.2, (c) 1.6, (d) 2.7, (e) 5.3, (f) 10.7, (g) 18.7, (h) 26.7, (i) 40.0, (j) 53.3, and (k) 80).

for free AC in dichloromethane. Normalization of the fluorescence intensity at 420 nm showed that the shape of the fluorescence spectra in the presence of TKS159 and TM166 changed. The fluorescence difference spectra at 25 °C (Figure 3) did not change shape as the template concentration was increased, suggesting that in the presence of each template the environment provided by the template does not change significantly when the concentration of template is raised. However, the difference spectra are not the same for TKS159 and TM166, indicating that AC is bound differently to each template. The same pattern for the difference of the normalized fluorescence spectra in the presence of TKS159 was seen at 0 °C, while at −25 °C a small deviation of the difference spectra was observed at low TKS/AC ratios (see Figure S6 in the Supporting Information). At −50 °C (Figure 4), the shape of the difference spectra changes as the concentration of TKS159 increased. The maximum observed above 500 nm shifts to shorter wavelengths as the TKS/AC ratio increases. This result suggests that at low TKS/AC ratios and low temperature a larger number of emissive species are available than at the higher temperatures studied.

Formation of AC hydrogen-bonded dimers has been proposed previously when the photodimerization reaction of AC in various solvents was investigated.[49] For this reason,

(49) Mizoguchi, J.; Wada, T.; Inoue, Y. *Chem. Lett.* **2006**, *35*, 738–739.

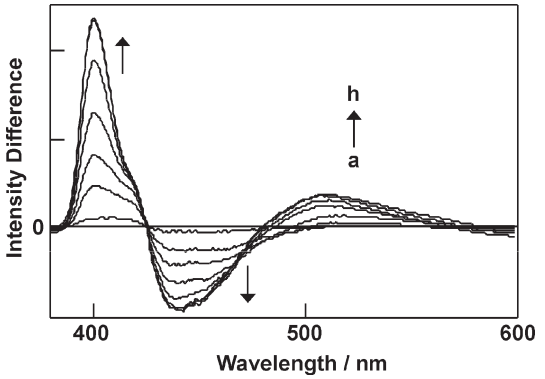

FIGURE 4. Difference spectra at −50 °C of the fluorescence spectra normalized at 420 nm for AC (0.025 mM) in the presence of varying amounts of TKS159 and the spectrum in the absence of TKS159 (TKS/AC ratios: (a) 0.16, (b) 0.56, (c) 0.8, (d) 1.0, (e) 1.2, (f) 1.6, (g) 10.6, and (h) 40).

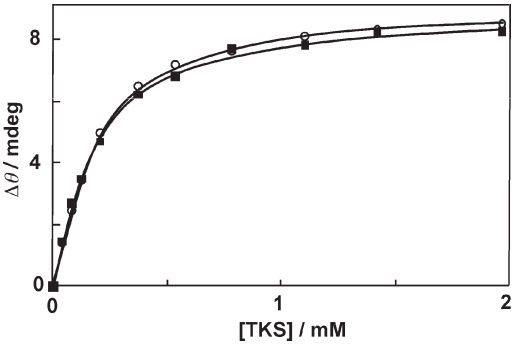

FIGURE 5. Plot of the change of ellipticity at 367 nm (solid square) and 386 nm (open circle) based on the CD titration at 10 °C of AC with TKS159. The solid line corresponds to the fit of the experimental data to a binding isotherm derived for a 1:1 stoichiometry when neither the AC nor the TKS159 concentrations are in excess (see the Experimental Section).

the changes in the difference spectra at −50 °C could be due to the formation of the AC hydrogen-bonded dimers. In order to explore this possibility, the fluorescence spectra for AC in dichloromethane at various AC concentrations were measured at different temperatures. The normalized fluorescence spectra for AC (2.5−75 μM) were the same at 25 and 0 °C, whereas a change was observed at 75 μM AC at −25 °C and above 6.25 μM AC at −50 °C (Figure S7 in the Supporting Information). The change in the AC fluorescence spectra at −50 °C as the AC concentration increases (Figure S7) suggests that a significant amount of AC is present in solution as an AC hydrogen-bonded dimer. Therefore, at low concentrations of TKS159 the difference spectra shown in Figure 4 correspond to changes in the AC monomer/hydrogen-bonded dimer ratio and the formation of the AC−TKS complex. At high TKS159 concentrations, the AC−TKS complex is the major species in solution. Unless otherwise stated, the following results represent experimental conditions for which the contribution of the AC hydrogen-bonded dimer in homogeneous solution is negligible.

Complex stability constant values can be determined by studying the changes in the intensities for the absorption, CD, or fluorescence spectra with an increase in the concentration of template. A 1:1 guest/template stoichiometry was assumed for these studies. The changes observed for the fluorescence intensities were due to various factors (see below), such as dynamic quenching of free AC by the host, in addition to the formation of the complex. For this reason, fluorescence data were not suitable for the determination of the AC−template complex stability constants. Absorption data are less precise because of the small changes observed for the absorption of AC in the presence of TKS, but the values of K recovered are the same within experimental error to the ones determined from CD data (see below).

The complex stability constant (K) values were determined from the changes in the induced CD intensity of AC (0.1 mM) with the increase in the concentration of TKS159 (Figure 5, Table 1). In the case of TM166 no induced CD signal was observed, and a competitive CD measurement was performed. TM166 was added to a solution containing sufficient TKS159 to bind over 97% of AC. The decrease in the AC−TKS CD signal is related to the amount of AC displaced to bind TM166, and this decrease is used to calculate the value of K for the AC−TM complex (Table 1).

TABLE 1. Stability Constants (K) for AC−TKS and AC−TM Complexes Determined by Direct (TKS159) or Competitive (TM166) Circular Dichroism Spectral Titration Experiments at Various Temperatures[a]

	K/M^{-1}	
T/°C	TKS159[b]	TM166[c]
25	3400 ± 200 (4)	1400 ± 100
10	7400 ± 400 (1)	3000 ± 200
0	15000 ± 1000 (1)	5800 ± 400

[a]Direct CD titrations were run by adding TKS159 to an AC/CH_2Cl_2 solution and fitting the data to a binding isotherm assuming a 1:1 stoichiometry. For each independent experiment, the K value was determined at two wavelengths (367 and 386 nm). Competitive CD titrations were performed by adding TM166 to an AC/TKS159 solution. The value for K was calculated from the decrease in the AC-induced CD signal. [b]For experiments performed once, the errors correspond to the error propagation for the values determined by the data fit at each individual wavelength. For experiments performed more than once, the errors correspond to standard deviations. Number of independent runs are shown in parentheses. [c]Errors correspond to error propagation from the averages for the competitive titration method and the error for K for TKS159.

The values of K increased as the temperature of the solution was lowered (Table 1). However, attempts to obtain values at −25 and −50 °C were hampered because of the unavailability of a suitable cooling system for the CD spectrometer. For this reason, the values of K at the low temperatures for a 1:1 complexation stoichiometry were estimated from the fit of the data at higher temperatures to the van't Hoff equation (eq 1) (Figure 6). The K values for AC−TKS were calculated to be $(9 \pm 1) \times 10^4$ M^{-1} and $(8 \pm 1) \times 10^5$ M^{-1} at −25 and −50 °C, respectively. It is important to note that this extrapolation to lower temperatures assumes that the complex stoichiometry is 1:1 and that no other types of complexes were formed. From the van't Hoff plots (Figure 6), the enthalpy ($\Delta H°$) and entropy changes ($\Delta S°$) were calculated for the 1:1 complex formation of AC with TM166 and TKS159 (Table 2).

$$\ln K = -\Delta H°/RT + \Delta S°/R \quad (1)$$

Job plots, based on the changes in the induced CD signals, were constructed at 25 and 0 °C ([AC]$_0$ + [TKS]$_0$ = 1 mM; see

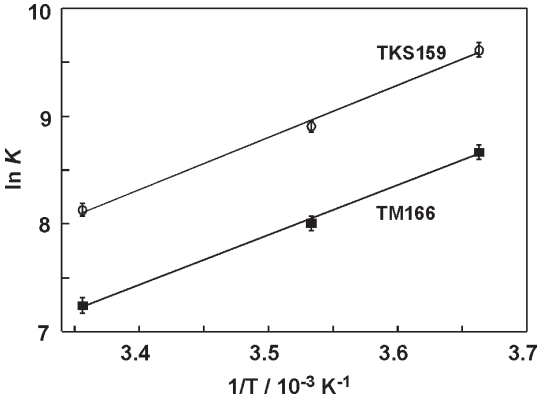

FIGURE 6. van't Hoff plots for AC−TM and AC−TKS complexation using the complex stability constants shown in Table 1.

TABLE 2. Thermodynamic Parameters for the Complexation of AC with Templates TKS159 and TM166 in Dichloromethane at $T = 298.15$ K[a]

template	$\Delta G°$/kJ mol^{-1}	$\Delta H°$/kJ mol^{-1}	$T\Delta S°$/kJ mol^{-1}
TKS159	−(20 ± 4)	−(40 ± 3)	−(20 ± 2)
TM166	−(18 ± 3)	−(37 ± 2)	−(19 ± 2)

[a]Errors correspond to statistical errors for the fit of the data to eq 1.

Figure S8 in the Supporting Information) to determine the stoichiometry of the complex between AC and TKS159. A maximum was observed at 0.5 indicating that the stoichiometry of the complex is 1:1. Measurements at [AC]/([AC] + [TKS]) ratios higher than 0.7 and at low temperatures were not possible because of the presence of an AC precipitate.

Fluorescence Lifetime Measurements. Kinetic measurements for the decay of the singlet excited state of AC in the presence of template are useful to obtain mechanistic information on the photodimerization reaction, provided that the lifetimes for AC free in dichloromethane and when bound to the templates are different. Control experiments using the methyl ester of AC (ACOMe) were performed to determine if the excited state of ACOMe could be dynamically quenched by the templates in a bimolecular reaction without the formation of a ground-state complex. The absorption spectrum of ACOMe did not change in the presence of TKS159, indicating that no complex was formed because ACOMe lacks the ability to form hydrogen bonds with the template. A shortening of the singlet excited state lifetime of ACOMe was observed in the presence of TKS159 and TM166 indicating that quenching occurred. A linear relationship was observed between the observed decay rate constant (k_{obs}) and the quencher concentration ([Q]). The quenching rate constants (k_q) were determined from the fit of the data to eq 2, where k_o corresponds to the inverse of the singlet excited lifetime of ACOMe in the absence of quencher.

$$k_{obs} = k_o + k_q[Q] \quad (2)$$

The values of k_q for the quenching of ACOMe by TKS159 decreased as the temperature was lowered: $(3.4 \pm 0.1) \times 10^9$ M^{-1} s^{-1} at 25 °C, $(2.8 \pm 0.1) \times 10^9$ M^{-1} s^{-1} at 0 °C, $(2.1 \pm 0.1) \times 10^9$ M^{-1} s^{-1} at −25 °C, and $(1.5 \pm 0.2) \times 10^9$ M^{-1} s^{-1} at −50 °C. The quenching rate constant of ACOMe by TM166 at 25 °C was determined to be $(3.1 \pm 0.1) \times 10^9$ M^{-1} s^{-1}. These quenching rate constants are almost 1 order of magnitude lower than the rate constant observed for a diffusion-controlled process in dichloromethane (1.6×10^{10} M^{-1} s^{-1} at 25 °C).[50] However, the k_q values are sufficiently high for the decrease observed at lower temperatures to be mostly due to an increase in the solvent viscosity. This quenching observed for ACOMe needs to be taken into account when analyzing the changes in lifetime for the AC/template systems.

TABLE 3. Fluorescence Lifetimes (τ) and Pre-exponential Factors (A) for AC−TKS Complexes at Various Temperatures[a]

T/°C	TKS/AC	AC bound[b] /%	τ_2[c]/ns	A_2[d]	τ_3[e] /ns	A_3[d]	A_2/A_3
25	80	87	3.7 ± 0.3	0.28[f]	10	0.69[f]	0.41 ± 0.03
0	40−80	≥94	3.9 ± 0.5	0.42[g]	12	0.58[g]	0.72 ± 0.04
−25	10.7−80	≥96	4.5 ± 0.3	0.54[g]	13	0.46[g]	1.18 ± 0.07
−50	10.7−80	≥99	6.1 ± 0.5	0.54[g]	18	0.46[g]	1.18 ± 0.07

[a]Measured in aerated CH_2Cl_2: [AC] = 0.025 mM; $\lambda_{ex} = 361$ nm; $\lambda_{em} = 440$ nm. [b]Calculated using the complex stability constants assuming a 1:1 binding stoichiometry (see text). [c]Average determined from the fit of the fluorescence decay to the sum of two exponentials. [d]Estimated errors ± 0.02. [e]Estimated when the concentration of AC free in dichloromethane was low (see text), estimated error ± 2 ns. [f]Determined from the fit of the decay to the sum of three exponentials. [g]Determined from the fit of the decay to two exponentials where the long-lived component is assigned exclusively to TKS159-bound AC.

The decay for AC in dichloromethane followed a monoexponential function (Figure S9 in the Supporting Information), and the lifetime of the singlet excited state of AC lengthened as the temperature was lowered from 25 °C (14.9 ns) to 0 °C (16.6 ns) and then leveled off at −25 °C (17.5 ns) and −50 °C (17.0 ns). The decay of the AC fluorescence in the presence of templates did not follow a monoexponential decay (Figure S9 in the Supporting Information). A shortening of the lifetime was observed, which is consistent with the decrease in the steady-state fluorescence intensity observed for the AC/template solutions. Adequate fits were obtained when fitting the decays to a sum of two exponentials. The pre-exponential factor (A_i) for each species is related to the concentration of that particular species, taking into account the species' excitation efficiency. The excitation efficiencies for free and bound AC were different and are unknown because the bandwidth for the single-photon-counting experiment was 16 nm. However, trends in the A_i values with changes in the concentration of TKS159 can be correlated with changes in concentration of each species.

The lifetime of the long-lived component at 25 °C decreased from 14.9 ns for AC free in dichloromethane to 10.7 ns when the TKS/AC ratio was 80. The short-lived component became more prominent as the concentration of TKS159 was increased (Table S1 in Supporting Information). Once the pre-exponential factor for the short-lived component was significant ($A_2 \geq 0.1$), the lifetime for this component was constant at 3.7 ± 0.3 ns (Table 3). This short-lived component, which is only present when AC is bound to TKS159, is assigned to a complex between AC and TKS159. The long-lived component incorporates the emission of AC free in dichloromethane; however, its lifetime was shorter than expected for the bimolecular quenching of AC by TKS159 based on the k_q values determined using ACOMe. For example, at a TKS/AC ratio of 80 the calculated

(50) Murov, S. L.; Carmichael, I.; Hug, G. L. *Handbook of Photochemistry*; 2nd, revised and expanded ed.; Marcel Dekker, Inc.: New York, 1993.

TABLE 4. Product Distribution and Enantiomeric Excess (ee) for the Photodimerization Reaction of AC in Dichloromethane in the Presence and Absence of TKS159[a]

				product distribution/%				% ee				
T/°C	TKS/AC	AC bound[b] /%	conv/%	**1**	**2**	**3**	**4**	**2**	**3**	HT/HH	anti/syn	(**1** + **4**)/(**2** + **3**)
25	0	0	92	33	22	24	21	1	0	1.2	1.3	1.2
	40	97	96	38	25	24	13	−28	−20	1.7	1.6	1.0
	120	> 99	97	40	26	23	11	−25	−23	1.9	1.7	1.0
0	0	0	60	36	20	28	16	−2	0	1.3	1.8	1.1
	28	> 99	95	39	27	24	10	−33	−28	1.9	1.7	1.0
−25	0[c]	0	12[d]	41	15	34	10	−3	0	1.3	3.0	1.0
	10	> 99	93	37	24	28	11	−37	−36	1.6	1.9	0.9
−30[e]	10	> 99	19	37	24	29	10	−39	−38	1.6	1.9	0.9
−40[e]	10	> 99	23	38	22	30	10	−41	−44	1.5	2.1	0.9
−50	0[c]	0	3[d]	33	13	39	15	2	−2	0.9	2.6	0.9
	3	> 99	88	41	19	31	9	−43	−49	1.5	2.6	1.0
	10	> 99	90	38	20	32	10	−42	−48	1.4	2.3	0.9

[a][AC] = 0.25 mM, unless noted otherwise. Irradiated at $\lambda \geq 320$ nm for 120 min, errors for product distribution ±1% and errors for ee values ±2%. [b]Calculated using the complex stability constants assuming a 1:1 binding stoichiometry (see text). [c]Precipitation of AC observed. [d]Low conversion due to the precipitation of AC. [e][AC] = 0.2 mM, irradiated for 30 min.

lifetime for free AC is 13.7 ns, while the measured lifetime was 10.7 ns. In addition, if the long-lived component was related to free AC the A_1 value should decrease as the concentration of TKS is raised, but the A_1 value levels off at 0.7. Both the excessive shortening of τ_1 and leveling off observed for A_1 suggest that another AC−TKS complex was present that had a longer lifetime than the species with the 3.7 ns lifetime.

The lifetime for the second AC−TKS complex was estimated by fitting the decays to the sum of three exponentials where the value of τ_1 was fixed to the value calculated for the lifetime of free AC, taking into account the dynamic quenching determined with ACOMe, and by fixing τ_2 to 3.7 ns (Table S1 in the Supporting Information). The lifetime of the second AC−TKS species (τ_3) is close to that for AC in dichloromethane. For this reason, fitting the decays to the sum of three exponentials, when a significant portion of the AC is free in solution, was not satisfactory, leading to A_1 and A_3 values that are theoretically not possible (Table S1 in the Supporting Information). However, at high TKS/AC ratios the values for A_1 are very low because most of the ACs are bound to the template. The values for τ_3, A_2, and A_3 at 25 °C were taken from the fit of the data to the sum of three exponentials at the highest TKS/AC ratio studied (Table 3).

The analysis of the decays at lower temperatures is facilitated because conditions could be used where most (≥90%) of the AC was bound to TKS159. At 0 and −25 °C, the value for τ_1 at high TKS/AC ratios was shorter than calculated from the dynamic quenching of the excited AC by the template (Tables S2 and S3 in the Supporting Information), again suggesting that a third emissive species was present. The fit to the sum of three exponentials is consistent with this assignment. However, the values for τ_3, A_2, and A_3 reported are those from the fit to the sum of two exponentials under conditions where most AC was bound (Table 3). At −50 °C, the two lifetimes changed little but the pre-exponential factors changed until constant values were observed when more than 90% of the AC was bound (Table S4 in the Supporting Information).

The two singlet excited state lifetimes for the AC−TKS complexes (see the Discussion for a structural assignment) were lengthened as the temperature was lowered. In addition, the concentration ratio between these two species, expressed as A_2/A_3, increased as the temperature was lowered from +25 to −25 °C but remained constant between −25 and −50 °C (Table 3).

The decays for the AC fluorescence at 0 °C for a TKS/AC ratio of 80 were measured at several wavelengths (395, 440, and 520 nm). The decays were fit to the sum of two exponentials because at this TKS159 concentration 97% of the AC is bound. The temperature of 0 °C was chosen because conditions could be used when almost all AC was bound to TKS159 and no AC hydrogen-bonded dimers were formed at the AC concentration employed (0.025 mM) (see above and Figure S7 in the Supporting Information). The two lifetimes recovered at these three wavelengths ranged from 3.5 to 4.1 ns and 11.0 to 11.4 ns, which are the same lifetimes as determined from multiple experiments at various TKS/AC ratios (see Table S2 in the Supporting Information). The pre-exponential factor for the short-lived species decreased from 0.64 at 395 nm to 0.43 at 440 nm and 0.12 at 520 nm, while the pre-exponential factors for the long-lived species increased from 0.36 to 0.57 and 0.88 as the detection wavelength became longer. This result suggests that the spectrum corresponding to the long-lived species is red-shifted compared to the spectrum for the short-lived species.

In the case of TM166 only an extended complex is formed with AC.[25] Two lifetimes were observed for the singlet excited state of AC in the presence of TM166 at 25 °C (Table S5 in the Supporting Information), and the τ_1 value was shortened from 14.9 ns in the absence of TM166 to 13.5 ns at a TKS/AC ratio of 80. The value calculated for τ_1 taking into account the dynamic quenching of excited AC by TM166 is 13.7 ns. This result shows that in the case of TM166 only one complex is formed with AC, which has a lifetime (5.0 ± 0.2 ns) shorter than the excited AC lifetime in dichloromethane. The lifetime for the complex increased from 5 ns at 25 °C to 9 ns at −25 °C and 10 ns at −50 °C.

Product Studies. The distribution of the four stereoisomeric products **1**−**4** and the ee values for chiral products **2** and **3** were determined by chiral HPLC for the photodimerization in the presence and absence of TKS159 at various temperatures (Table 4).

In the absence of TKS159, the solubility of AC in dichloromethane is limited, particularly at lower temperatures, and a solution of 0.25 mM AC forms precipitates at temperatures below −25 °C. For this reason, the photodimerization of AC

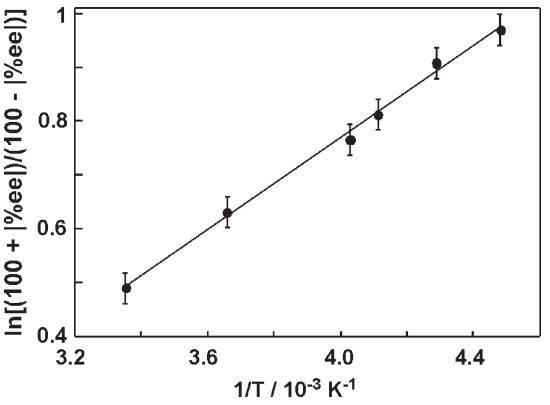

FIGURE 7. Eyring plot of the enantiomer ratio obtained upon irradiation at various temperatures (data from Table 3).

alone was seriously decelerated to give extremely low conversions (3−12%) at low temperatures. However, the addition of an excess amount of TKS159 readily solubilized AC of 0.25 mM in dichloromethane, even at −50 °C.

Control experiments at +25, −25, and −50 °C showed that the product distribution (±1% error), and the ee values (±2% error) were independent of the conversion and the AC concentration (0.05−0.25 mM, Table S6 in the Supporting Information). This result is important because the fluorescence lifetime measurements were performed at low AC concentrations (0.025 mM), while the product studies were normally performed at higher concentrations (0.25 mM) to increase the precision of the HPLC analysis.

As shown in Table 4, in the presence of TKS159 the formation of HT dimers **1** and **2** was appreciably increased at the expense of HH dimers **3** and **4** at all temperatures studied. This probably reflects the fact that the TKS159 hydrogen bonding to the carboxyl group (H-bonding end of the molecule) increases the *head-to-head* steric repulsion when these groups are aligned in the formation of the dimer. Once all AC molecules were bound to TKS159 the ee values for **2** and **3** did not change within the experimental error at each temperature examined. The ee values were gradually enhanced as the temperature was lowered and reached values of −43% and −49% at −50 °C. It is interesting to note that the (**1** + **4**)/(**2** + **3**) ratio is surprisingly constant around unity (1.0 ± 0.1), irrespective of the reacting species present in solution (free AC and AC−TKS complex), the temperature, and the conversion. This result is in sharp contrast to the behavior of HT/HH and anti/syn ratios and suggests the presence of a common precursor/process for each pair of photodimers (see below).

The increase in the magnitude of the ee as the temperature is lowered can be used to calculate an apparent differential enthalpy and entropy for the chirogenesis induced by complexation of AC to TKS159. It is important to note that these values can include a difference in the population of precursors, i.e., different equilibrium constants, and a difference in the reactivity of each complex. Therefore, this Eyring plot does not provide mechanistic information, but it can be used to establish whether the mechanism changes as the temperature is varied. We assume that the ee values for **2** and **3** are the same when more than 99% of AC is bound, and therefore, we used the average values to construct the Eyring plot (eq 3, Figure 7). The apparent differential enthalpy and entropy changes are $\Delta\Delta H = -(3.6 \pm 0.1)$ kJ mol^{-1} and $\Delta\Delta S = -(7.9 \pm 0.4)$ J mol^{-1} K^{-1}. The linearity of the Eyring plot suggests that the same mechanism operates at high and low temperatures.

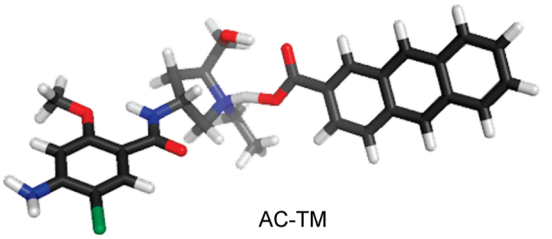

FIGURE 8. Structure of the AC−TM complex optimized by DFT-D-B-LYP/TZVP.

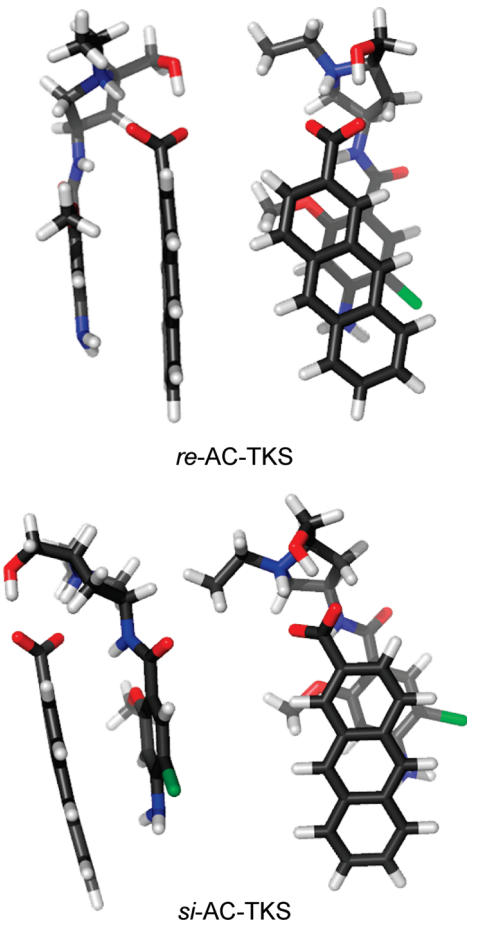

FIGURE 9. Structures of the *re*- and *si*-AC−TKS complexes optimized by DFT-D/B-LYP/TZVP, where the AC *re*- or *si*-face is accessible.

$$\ln \frac{(100+|\%ee|)}{(100-|\%ee|)} = \ln \frac{k}{k''} = \frac{\Delta\Delta S}{R} - \frac{\Delta\Delta H}{R}\frac{1}{T} \qquad (3)$$

DFT-D-Optimized Structures of AC−TKS and AC−TM Complexes. As a consequence of the prochiral nature of AC, the hydrogen-bonding interaction of AC with chiral template TKS159 leads to the formation of a pair of diastereomeric complexes, where either the *re*- or *si*-face of AC (the enantioface is defined at the 2-position of AC, to which the carboxylic group is attached) is shielded by

TABLE 5. Results of the DFT-D Calculations for AC−TM and *re*- and *si*-AC−TKS Complexes

		distance/Å				
complex	energy[a] /kJ mol^{-1}	O−H···O	N−H···O	Cl−AC[b]	face-to-face[c]	tilt angle[d] (deg)
AC−TM	38.4	1.612	1.465	11.16	13.34	59.6
re-AC−TKS	≡0.0	1.658	1.593	3.60	3.72	4.3
si-AC−TKS	8.6	1.651	1.607	4.67	4.10	12.1

[a] Energy relative to the most stable *re*-AC−TKS complex (for the detailed results including the actual energy, see the Supporting Information). [b]Distance between the chlorine atom of the template and the closest carbon atom of AC. [c]Center-to-center distance between the anthracene and the benzene ring of the template. [d]Tilt angle of the anthracene plane and the benzene plane of the template.

the methoxybenzamide moiety of TKS159. These conformations are folded, and there is no possibility for the direct interconversion between the *si* and *re* complexes without decomplexation of AC from the template. Epimeric TM166 also forms a pair of diastereomeric complexes with AC, which possess the extended conformation, as revealed by X-ray crystallography.[25] Hence, there will be no difference in stability between the two diastereomeric complexes, which can interconvert by free rotation around the bond between the aromatic ring and the carbon on the carboxyl group to spontaneously "racemize". As a consequence, no enantiodifferentiation in the products is observed, as demonstrated previously.[25]

Structure optimizations by the dispersion-corrected DFT-D method at the B-LYP level, which is known to appropriately correct for stacking interactions,[51] were performed for two diastereomeric AC−TKS complexes and an extended AC−TM complex. All structures were treated as the pyrrolidinium(TKS/TM)-carboxylate(AC) ion pair, as the X-ray crystallographic study revealed that the AC−TM complex exists in this salt form.[25] The DFT-optimized structure of the AC−TM complex (Figure 8) nicely reproduced the geometry of the structure obtained from X-ray crystallography justifying the geometry optimization at the DFT-D/B-LYP level for this kind of hydrogen-bonded complex. The DFT-optimized structures of diastereomeric *re*- and *si*-AC−TKS complexes have stacked conformations, in which the π overlap and the tilt angle between the two aromatic planes are appreciably different (Figure 9). The calculated energies and some selected geometries of the AC−TM and two AC−TKS complexes are summarized in Table 5.

Discussion

TKS159 and its epimer TM166 were previously shown to form complexes with AC. The enantiomeric excess for the photodimerization of AC observed for the AC−TKS complex is due to the shielding by the template of one of the faces of AC.[25] X-ray crystallographic studies, as well as NMR experiments, showed that the carboxylic group on AC forms two hydrogen bonds with the pyrrolidine nitrogen and the hydroxyl group of the templates. In the case of TKS159, the AC aromatic ring is partially covered by the 2-methoxybenzoyl moiety of the template. In contrast, for TM166, no such stacking occurs due to the 2*S*,4*R* configuration of the 4-aminoprolinol moiety.[25]

The blue shift observed in the absorption spectra of AC when bound to TKS159 and TM166 suggests that the carboxyl group on AC is partially deprotonated as expected from the formation of a hydrogen bond with the template. Deprotonation is not complete since the blue shift in the AC−TKS spectrum compared to the protonated AC is smaller than that observed for the spectrum of AC in the presence of triethylamine, where AC is deprotonated. The environment around AC is different in the complexes with TKS159 and TM166. AC complexation to TKS159 leads to strong induced CD signals, while no such signals were observed for the AC−TM complex. In addition, the fluorescence difference spectra are different for AC bound to TKS159 or TM166.

The driving force for the formation of the AC complex with TKS159 or TM166 is enthalpic, while an entropy loss, arising from the loss of degrees of freedom upon molecular association, is observed in both cases (Table 2). The $\Delta H°$ and $\Delta S°$ values are similar for both complexes. For the AC−TM complex, which has an extended conformation, the hydrogen-bonding interaction is the only source of enthalpic gain, while for the AC−TKS complex hydrogen bonding and $\pi-\pi$ stacking can lead to the stabilization of the complex. The two diastereomeric *re* and *si* complexes of TKS159 with AC are expected to be different in energy and geometry, while the TM166 complex will have conformers with similar energy since bond rotation is not restricted (see above). DFT-D calculations provide a qualitative estimate of the relative stability of these complexes (Table 5). The calculations predict that the AC−TM complex is less stable than the AC−TKS complexes in line with the equilibrium constant values determined from CD measurements (Table 1). The AC−TM complex has shorter hydrogen bonds than calculated for the two AC−TKS complexes by 0.04−0.05 Å for the OH···O distance and by 0.13−0.14 Å for the NH···O distance. The elongation of the hydrogen bonds in the case of TKS159 is likely to be driven by the structural demand of the TKS159 template but is energetically compensated by the π-stacking of two aromatic moieties in the AC−TKS complexes. An additional difference for the *re*- and *si*-AC−TKS complexes is the distance and tilt angle of the two aromatic rings in each complex (Table 5). Thus, the two aromatic rings in the *re* complex are closer (distance: 3.72 Å versus 4.10 Å) and more parallel to each other (tilt angle: 4.3° versus 12.1°) than those in the *si* complex, rendering the *re* complex more stable than the *si* complex. It is important to note that we could not differentiate the *K* values for the *re* and *si* complexes when determining the binding isotherm in the CD experiments. This result suggests that the difference between K_{re} and K_{si} is small and the overall *K* value incorporates the equilibrium constants for both complexes. In addition, the shape of the fluorescence difference spectra did not change for different TKS/AC ratios, suggesting that a similar proportion of *re*-AC−TKS and *si*-AC−TKS was present at all

(51) Grimme, S.; Antony, J.; Schwabe, T.; Muck-Lichtenfeld, C. *Org. Biomol. Chem.* **2007**, *5*, 741–758.

TKS/AC ratios. The time-resolved experiments established that the spectra for *re*-AC−TKS and *si*-AC−TKS are slightly different, and a change would have been observed for the steady-sate fluorescence difference spectra as the TKS/AC ratio was changed if the ratio for the concentration of the *re*- and *si*- complexes changed significantly.

The photophysics of anthracenes is very sensitive to substitution on the aromatic ring and the nature of the solvent, and therefore, the structural differences for the *re*-AC−TKS and *si*-AC−TKS complexes affect the lifetime of the singlet excited state of AC in each complex. The sensitivity of the photophysics of anthracenes is due to the closeness in energy of the S_1 and T_2 states.[52−56] Very small changes in the energies of S_1 or T_2 lead to significant variations in the intersystem crossing rate constants which directly affect the anthracene fluorescence quantum yields and singlet excited-state lifetimes. In addition, anthracenes can show dual emission resulting from the interconversion between conformational isomers.[57−60] This interconversion leads to the detection of coupled kinetics where growth kinetics are observed at certain wavelengths indicating the isomerization to the most stable conformer.

The shortening of the singlet excited state lifetime for AC bound to TM166 suggests that the lifetime of AC is sensitive to the degree of hydrogen bonding on the carboxyl group. It is important to note that in the AC−TM complex no π-stacking occurs, and therefore, π-stacking is not responsible for the shortening of the AC lifetime. In the case of TKS159, the two diastereomeric complexes have different singlet excited-state lifetimes, which are shorter than the lifetime for AC in dichloromethane. However, only one of the lifetimes is shorter than the one observed for AC−TM, while the second lifetime is longer. The different lifetimes for *re*-AC−TKS and *si*-AC−TKS are not likely due to differences in the degrees of hydrogen bonding because the calculated distances for the hydrogen bonds are similar in both complexes (Table 5). The structural differences between *re*-AC−TKS and *si*-AC−TKS are the degree of $\pi-\pi$ stacking and the distance between the AC aromatic ring and the Cl atom. The chlorine atom is expected to enhance the intersystem crossing quantum yield through a heavy atom effect decreasing the lifetime of the singlet excited state. Indeed, the singlet excited-state lifetimes of 1-chloro- and 2-chloroanthracene are shorter than the lifetime for anthracene.[53] Based on these considerations, we assign the shorter lifetime to the *re*-AC−TKS complex where the anthracene moiety is in closer proximity to the chlorine atom and the overlap of the aromatic systems is larger.

The observation of two lifetimes could in principle indicate the interconversion between two isomers, in this case the *si* and *re* complexes. However, such a mechanism would require the dissociation of the complex during the singlet excited-state lifetime of AC in order for bond rotation to occur around the bond between the aromatic ring and the carbon on the carboxyl group. The upper limit at 25 °C for the dissociation rate constant of the AC−TKS complex is 4.7×10^6 s^{-1}, which was calculated from the complex stability constant of 3400 M^{-1} and the diffusion rate constant in dichloromethane of 1.6×10^{10} M^{-1} s^{-1}. Complete dissociation is too slow compared to the decay of the species with the shortest lifetime (2.7×10^8 s^{-1}). In addition, no growth kinetics of the long-lived and red-shifted fluorescent species were observed, a result that eliminates the possibility of partial dissociation of AC and bond rotation during the excited state lifetime. Therefore, the lifetimes observed for the complex of AC with TKS159 are the intrinsic lifetimes of the individual *si* and *re* complexes. A quantitative analysis relating the pre-exponential factors with concentration ratios for the *re*-AC−TKS and *si*-AC−TKS is not warranted because the emission spectra for each complex are not known and the relative emission quantum yield at different wavelengths cannot be established. However, the trend that the pre-exponential factor for the short-lived species at 440 nm increases as the temperature is lowered is in agreement with the assignment of the short-lived species to the most stable *re*-AC−TKS complex.

Preliminary product studies at template/AC ratios of 10 using TKS159, TM166, and their enantiomers showed that AC complexation to TM166 did not lead to any significant changes in the distribution for products **1**−**4**, and no significant ee was observed.[25] Therefore, the complexation of AC to TM166 does not affect the photodimerization selectivity showing that the approach to the two faces of the AC bound to TM166 is the same as observed for AC in dichloromethane. In contrast, an ee was observed for products **2** and **3** for AC in the presence of TKS159. The magnitude of the ee values were the same for TKS159 and its enantiomer, but the signs were opposite showing that antipodal products were formed for each of the enantiomers.[25]

The ideal experimental conditions to gain mechanistic information for this system are those where the amount of AC in solution is minimized and the contribution of AC hydrogen-bonded dimers in solution is negligible. Binding of 99% of the AC was achieved at TKS/AC ratios of 120 at 25 °C, while complete binding was achieved at 0 °C for TKS/AC ratios of 28 or higher. At −25 and −50 °C, formation of hydrogen-bonded AC dimers occurred at the AC concentrations employed for product studies (0.25 mM) and low TKS159 concentrations. However, 99% of the AC was bound to the template when the TKS/AC ratio was 6 or higher at −25 °C and 3 or higher at −50 °C, and for these conditions no interference from the hydrogen-bonded AC dimer occurred for the product studies.

The two faces of AC are prochiral, and the stereochemistry of the products depends on which faces interact in the encounter complex. Interaction of an AC *re*-face with an AC *si*-face leads to the formation of achiral products **1** and **4**, while the interaction of ACs through *re*−*re* or *si*−*si* faces leads to chiral products **2** and **3** (Figure 10). The products formed from the *re*−*re* interaction are the enantiomers of the

(52) Bennett, R. G.; McCartin, P. J. *J. Chem. Phys.* **1966**, *44*, 1969–1972.
(53) Bohne, C.; Kennedy, S. R.; Boch, R.; Negri, F.; Orlandi, G.; Siebrand, W.; Scaiano, J. C. *J. Phys. Chem.* **1991**, *95*, 10300–10306.
(54) Kellogg, R. E. *J. Chem. Phys.* **1965**, *43*, 411–412.
(55) Lim, E. C.; Laposa, J. D.; Yu, J. M. H. *J. Mol. Spectrosc.* **1966**, *19*, 412–420.
(56) Ware, W. R.; Baldwin, B. A. *J. Chem. Phys.* **1965**, *43*, 1194–1197.
(57) Albrecht, M.; Bohne, C.; Granzhan, A.; Ihmels, H.; Pace, T. C. S.; Schnurpfeil, A.; Waidelich, M.; Yihwa, C. *J. Phys. Chem. A* **2007**, *111*, 1036–1044.
(58) Brearley, A. M.; Flom, S. R.; Nagarajan, V.; Barbara, P. F. *J. Phys. Chem.* **1986**, *90*, 2092–2099.
(59) Flom, S. R.; Nagarajan, V.; Barbara, P. F. *J. Phys. Chem.* **1986**, *90*, 2085–2092.
(60) Furuuchi, H.; Arai, T.; Sakuragi, H.; Tokumaru, K.; Nishimura, Y.; Yamazaki, I. *J. Phys. Chem.* **1991**, *95*, 10322–10325.

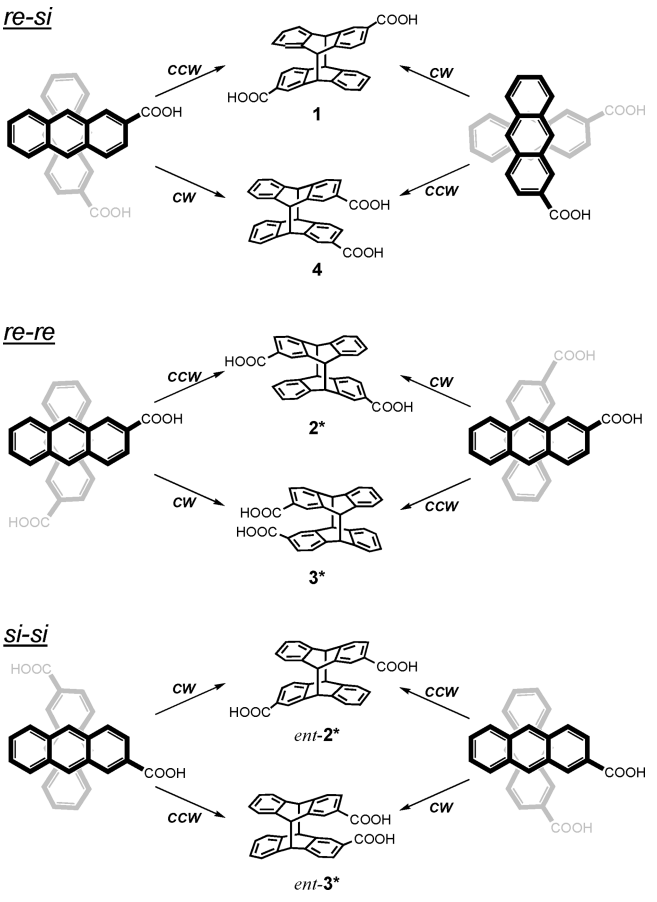

FIGURE 10. Product formation from the encounter complexes of two AC molecules assuming an "average" perpendicular geometry. CW and CCW indicate the clockwise and counterclockwise rotation of the top AC leading to the photodimer product. *Si* and *re* indicate the faces of the AC involved in the formation of the photodimer.

products formed from the *si*−*si* interactions. Therefore, the sum of products **1** and **4** compared to the sum of **2** and **3** indicates if the encounter complex involved opposite or the same prochiral faces of AC. A (**1** + **4**)/(**2** + **3**) ratio of 1 is expected in homogeneous solution if the reactivity of *re*−*si* encounter complexes is the same as the reactivity for the *re*−*re* and *si*−*si* encounter complexes. This ratio was 1.2 at 25 °C and 1.0 at 0 °C. Steric or electrostatic repulsion could affect the reactivity for photodimerization in two different ways. The repulsive interactions can lead to a higher dissociation of an encounter complex, therefore leading to a decreased reactivity for certain encounter geometries. The second effect is that the distribution between **1** and **4** and between **2** and **3** is dictated after an encounter complex is formed; i.e., the formation of the photodimer with higher repulsive interactions is minimized. The fact that the (**1** + **4**)/(**2** + **3**) ratio is close to unity indicates that repulsive effects play only a minor role at least in the early stages of the encounter complex. For this reason, we propose that the encounter complexes on "average" have a perpendicular geometry, where electrostatic repulsion is minimized (Figure 10). The formation of the products is then determined by the relative rotation of the two AC molecules.

Analysis for the product distribution and ee values at TKS159 concentrations when all AC is bound has to take into account the *re*- and *si*-AC−TKS complexes but does not have to include any reactivity of free AC since the concentration of the latter species is negligible. The photoreaction was carried out under zero-order conditions, where the concentration of excited states was much lower than the concentration of reagents and the illumination was constant. The reaction of the singlet excited state of the *re*-AC-TKS complex (*re**) and of the singlet excited state of the *si*-AC−TKS (*si**) can be seen as parallel reactions where *re** and *si** are two different reagents that reacted with either the ground-state complexes *re* or *si*. Re-equilibration between *re* and *si* occurred in the ground state because the lifetimes of *re** and *si** were short. Therefore, throughout the reaction the ratio [*re*]/[*si*] was constant and was determined by the equilibrium constants in the ground state of AC with TKS159. The probability of the formation of the four possible complexes, i.e., *re**−*si, si**−*re*, *re**−*re*, and *si**−*si*, remains constant during the reaction because ground-state re-equilibration between *re* and *si* occurred. This analysis is consistent with the fact that the product distribution does not change with the irradiation time, i.e., with the degree of conversion of the reactant. A further consequence of this analysis is that the ee can be used as a measure of the ratio for the concentrations of the *re* and *si* complexes because the fraction of complexes reacting through the *re**−*si* and *si**−*re*, leading to nonchiral products **1** and **4**, will be constant throughout the photoreaction.

Products **2** and **3** are formed from the encounter complexes *re**−*re* and *si**−*si*, where one of the encounter complexes leads to the formation of products $\mathbf{2}_-$ and $\mathbf{3}_-$ while the other encounter complex leads to the formation of products $\mathbf{2}_+$ and $\mathbf{3}_+$. We assigned the short-lived AC−TKS species to the *re* complex because calculations showed that this complex was more stable than the *si*-AC−TKS complex, and as the temperature was lowered the pre-exponential factors for the short-lived species increased. The ee increased as the temperature was lowered indicating that it arises from the complex with the short lifetime, and therefore, products $\mathbf{2}_-$ and $\mathbf{3}_-$ are formed from the *re**−*re* encounter complex, leading to the negative ee observed in the product studies (note that the "−" and "+" signs are arbitrary and are related to the elution time from the HPLC column, "+" being assigned to the product that elutes first).

The ee values are determined by the relative amounts of the *re* and *si* complexes, the intrinsic reactivity for photodimerization, and the lifetimes of *re** and *si**. A very different intrinsic reactivity for the *re**−*re* and *si**−*si* encounter complexes, which are diastereomeric in the presence of chiral template TKS159, would lead to a different partition between products **2** and **3** for each complex leading to different values for the ee of **2** and **3**. The similar ee values observed at each temperature suggests that the partition for the formation of **2** and **3** is similar in the *re**−*re* and *si**−*si* encounter complexes. Therefore the major discriminating factors leading to the chirogenesis observed are the relative amount of the *re* and *si* complexes and the lifetimes for each complex (τ_{re} and τ_{si}). The product ratio from the *re**−*re* and *si**−*si* encounter complexes are related to the ratio of encounter complexes, which in turn is related to the concentration of excited states, the

excited-state lifetimes, and the concentrations of ground states (eq 4).

$$\frac{[2_-+3_-]}{[2_++3_+]} = \frac{[re^*-re]}{[si^*-si]} = \frac{\tau_{re}[re^*][re]}{\tau_{si}[si^*][si]} \quad (4)$$

The ratio of excited states is equal to the ground-state ratio for the *re* and *si* complexes (see above) leading to a squared dependence of the product ratio:

$$\frac{[2_-+3_-]}{[2_++3_+]} = \frac{\tau_{re}[re]^2}{\tau_{si}[si]^2} \quad (5)$$

Qualitatively, the ee observed is due to a [*re*]/[*si*] ratio larger than unity because the lifetime for the *re* complex is shorter than for the *si* complex. The [*re*]/[*si*] ratio cannot be calculated from the pre-exponential factors recovered from the time-resolved experiments because the emission efficiency and the spectra for each complex are unknown. However, this ratio can be calculated from the ee values observed (eq 6).

$$\frac{[2_-+3_-]}{[2_++3_+]} = \frac{100+|\%ee|}{100-|\%ee|} \quad (6)$$

Combining eqs 5 and 6 leads to

$$\frac{\tau_{re}[re]^2}{\tau_{si}[si]^2} = \frac{100+|\%ee|}{100-|\%ee|} \quad (7)$$

The average ee values for **2** and **3** were used to calculate the [*re*]/[*si*] ratio (Table 6), which as expected increased as the temperature was lowered. The ee values are decreased by the shorter excited-state lifetime for *re*-AC−TKS compared to the *si* complex. The diastereomeric excess for the *re* and *si* complexes were calculated as well as the ee values assuming equal lifetimes for the *re* and the *si* complexes (|ee′|) (Table 6). It is important to emphasize the inherent advantage of the enantiodifferentiating photodimerization for a bimolecular reaction because the product ee can be much larger than the diastereomeric excess due to the dependence of the ee on the square of the concentration ratio for the *re* and *si* complexes. The ee can be further enhanced by a strategy where the lifetime of the most stable complex is designed to be longer than the lifetime of the least stable complex, the opposite situation from that observed for TKS159. Our results clearly showed for the first time that the product's enantiomeric excess (ee) is not simply determined by the diastereomeric ratio of the ground-state complexes but also depends on the relative lifetimes of the diastereomeric complexes. Therefore, the future rational design of supramolecular systems to achieve photochirogenesis should consider thermodynamic factors, such as the stability of complexes, and kinetic factors, such as the lifetime of excited states.

In conclusion, we have established a protocol, which should become standard, to fully elucidate the mechanism for photochirogenesis in supramolecular systems. The full characterization, i.e., spectral features, lifetimes and relative abundance, of two distinct excited state diastereomeric complexes was achieved for the first time by combining lifetime and product studies. These comprehensive studies revealed the importance of understanding the ground state behavior of the system, i.e., differential complex stability, combined with kinetic behavior of the excited states providing detailed information on the mechanism and stereochemical consequences of the photodimerization reaction.

TABLE 6. Calculations of *re*/*si* Ratio and the Diastereomeric Excess (de) upon Complex Formation and the ee′ Obtained When the *re* and *si* Complexes Have the Same Lifetime[a]

	obsd			calcd		
T/°C	τ_{re}/ns	τ_{si}/ns	|ee|/%	[*re*]/[*si*][a]	de/%	|ee′|/%
25	3.7	10	24	2.1 ± 0.5	35	63
0	3.9	12	30.5	2.4 ± 0.5	41	70
−25	4.5	13	36.5	2.5 ± 0.4	43	72
−50	6.1	18	45	2.8 ± 0.4	47	77

[a]Errors correspond to the error propagation for the lifetimes (Table 3) and ±2% for the ee values.

Experimental Section

Materials. 2-Anthracenecarboxylic acid, triethylamine (99% checked by GC), and dichloromethane (fluorescence grade) were used as received. Acetonitrile was purchased from Wako (HPLC grade) or from Kanto (purified by distillation). 4-Amino-5-chloro-2-methoxy-*N*-[(*2S,4S*)-1-ethyl-2-hydroxymethyl-4-pyrrolidinyl]benzamide (TKS159) and 4-amino-5-chloro-2-methoxy-*N*-[(*2S,4R*)-1-ethyl-2-hydroxymethyl-4-pyrrolidinyl]-benzamide (TM166) were prepared as previously reported.[47] 2-Anthracenecarboxylic acid methyl ester (ACOMe) was synthesized in 94% yield by the reaction of 2-anthracenecarboxylic acid (0.5 g, 2.25 mM) in dry methanol (30 mL) containing sulfuric acid (1 mL) at 65 °C and the subsequent workup and column chromatography on silica gel with a chloroform eluent (see Figure S10 in the Supporting Information for ^{1}H NMR). This assignment is in agreement with the published characterization of this compound.[61]

Equipment. Circular dichroism (CD) spectra were measured on a JASCO J-820S instrument equipped with an ETC505T temperature controller. Fluorescence spectra were collected with a JASCO FP6500 spectrometer, and samples were kept at a constant temperature with a Unisoku cryostat (USP-203HP model). The bandwidths for the emission and excitation slits were set to 3 and 1 nm, respectively. An excitation wavelength of 361 nm was used for measurements at 25, 0, and −50 °C, and 362.5 nm was used for measurements at −25 °C. The emission spectra were collected between 380 and 600 nm.

Fluorescence decays were measured with Edinburgh Instruments OB 920 or FL 920S single-photon counters using a hydrogen-filled ns-flash lamp as the excitation light source. The bandwidth was approximately 16 nm for both the excitation and emission monochromators. The maximum intensity collected was 2000 counts. The excitation and emission wavelengths were 361 and 440 nm, respectively. The excitation and emission monochromators were set to the excitation wavelength of the sample in order to collect the instrument response function (IRF) using the scattered light from an aqueous solution containing suspended silica gel. For temperatures at or below 0 °C, the IRF was collected using a dichloromethane solution instead of the aqueous solution. The decays were fit to an exponential function ($i = 1$) or to a sum of exponentials (eq 8) using software from the manufacturer to deconvolute the IRF from the experimental data.

$$I(t) = I_o \sum_1^i A_i e^{-k_i t} \quad (8)$$

The parameter A_i corresponds to the pre-exponential factor for each emissive species, i, with a different lifetime, where the

(61) Kriegel, R. M.; Saliba, K. L.; Jones, G.; Schiraldi, D. A.; Collard, D. M. *Macromol. Chem. Phys.* **2005**, *206*, 1479–1487.

sum of all pre-exponential factors is equal to 1. The parameter k_i corresponds to the decay rate constant of each fluorescent species, and its inverse value is equal to the singlet excited state lifetime of the emissive species. The fit of the experimental data to eq 8 was considered to be acceptable when the χ^2 value was between 0.9 and 1.2. Visual inspection of the residuals and autocorrelation was also used to determine the quality of the fit.[62]

A 500-W ultrahigh pressure mercury lamp fitted with a UV-35 filter (effective $\lambda > 320$ nm) was used for the photoreaction experiments. Temperature was controlled using a Unisoku cryostat (USP-203HP model). The HPLC system was equipped with a tandem column of Cosmosil 5C18-AR-II (Nacalai Tesque) and Chiralcel OJ-RH (Daicel). The eluent was a 64:36 (v/v) mixture of water and acetonitrile, the latter containing 0.1% trifluoroacetic acid. The rate of flow was 0.5 mL min^{-1}, and 5 μL aliquots of sample were injected. The columns were kept at 35 °C. The relative yield and %ee were determined from the peak areas on the HPLC chromatogram observed by the fluorescence detector (λ_{ex} = 254 nm, λ_{em} = 420 nm). This detection method relies on the photodecomposition of the AC photodimers by the excitation light, the efficiency of which was confirmed to be identical for all photodimers, followed by the excitation of the AC monomers produced in the detection cuvette.[63]

Sample Preparation. AC stock solutions (approximately 1 mM) were prepared by dissolving AC in dichloromethane with sonication. The actual AC concentration was determined by UV/vis ($\varepsilon_{397} = 4100$ M^{-1} cm^{-1}). TKS159 or TM166 stock solutions (4.0, 20, or 60 mM) were prepared by dissolving each template in dichloromethane. TM166 is less soluble than TKS159, and the stock solutions of TM166 were sonicated to achieve solubilization. Solutions for UV/vis, CD, and fluorescence experiments were made in dichloromethane by adding the appropriate amounts of AC and template stock solutions, with the exception of the UV/vis experiments at template/AC ratios above 20, where solid TKS159 was added to the solutions to avoid excessive dilution of AC. The concentrations used for UV/vis and CD experiments were [AC] = 0.1 mM, [template] = 0.02−12 mM ([template]/[AC] = 0.2−120), and the concentrations used for fluorescence experiments were [AC] = 0.025 mM, [template] = 0.0125 − 2 mM ([template]/[AC] = 0.5 − 80). All UV/vis, CD, and fluorescence solutions were aerated.

Solutions for photoreactions were prepared by mixing 2 mL of 0.5 mM AC with 2 mL of a TKS159 solution (0.125−60 mM) to obtain reaction mixtures with [AC] = 0.25 mM, [TKS] = 0.0625−30 mM (TKS/AC = 0.25−120). Solutions were placed in $1 \times 1 \times 4.5$ cm quartz cells containing a stirrer and sealed with septa. Solutions were deoxygenated by cooling on ice and bubbling Ar for at least 5 min. Solutions were stirred during the photoreactions. After photoirradiation, the dichloromethane was evaporated to leave an organic residue, which was redissolved in 4 mL of a 1:1 mixture of aqueous NaOH (2 mM) and acetonitrile. This mixture was used for the HPLC analysis.

UV/vis, CD, and Fluorescence Spectral Titration. Spectra were measured upon gradual addition of a TKS159 stock solution to 3 mL of AC solution. UV/vis and CD spectra were recorded at the various TKS/AC ratios at 25, 10, and 0 °C. Fluorescence spectra and decays were obtained at 25, 0, −25, and −50 °C. The maximum volume of added TKS159 was 300 μL. The measured absorbance and ellipticity values were corrected for dilution.

Determination of the Complex Stability Constants. The complex stability constants were determined using a nonlinear least-squares method based on the CD spectral changes upon titrating TKS159 solutions with AC. The titration curves were fit (eq 9) using KaleidaGraph. A 1:1 equilibrium was assumed between AC and TKS159. Neither species is in excess, resulting in the solution for a quadratic equation

$$\Delta\theta = \frac{\alpha}{[AC]_0}\frac{([AC]_0+[TKS]_0+1/K) \pm \sqrt{([AC]_0+[TKS]_0+1/K)^2 - 4[AC]_0[TKS]_0}}{2} \quad (9)$$

where $\Delta\theta$ is the change in ellipticity, K is the complex stability constant, $[AC]_0$ and $[TKS]_o$ are the initial concentrations of AC and TKS159, and α is the maximum ellipticity when all AC is bound.

Competition Experiments. Competition experiments for the binding of AC with TM166 and TKS159 were performed because AC binding to TM166 did not lead to a CD signal. Two 0.1 mM AC solutions, containing TKS159 (12 mM) or TKS159 (12 mM) + TM166 (12 mM), were prepared, and their CD spectra were measured at 25, 10, and 0 °C. Under these conditions, >97% of added AC are bound to a template.

The solution containing just TKS159 leads to an ellipticity value when all AC is bound to TKS (θ_{TKS}), while the observed ellipticity (θ_{obs}) in the presence of TKS159 and TM166 is decreased by the amount of AC bound to TM166. The ratio of equilibrium constants is given by eq 10, while the ratio of complexed AC to each template is calculated from eq 11, and the free concentration of TKS159 and TM166 are calculated from the mass balance eqs 12 and 13, where the subscript "T" corresponds to total concentrations.

$$\frac{K_{TKS}}{K_{TM}} = \frac{[AC\cdot TKS][TM]}{[AC\cdot TM][TKS]} \quad (10)$$

$$\frac{[AC\cdot TKS]}{[AC\cdot TM]} = \frac{\theta_{obs}}{\theta_{TKS} - \theta_{obs}} \quad (11)$$

$$[TKS] = [TKS]_T - [AC]_T \times \frac{\theta_{obs}}{\theta_{TKS}} \quad (12)$$

$$[TM166] = [TM166]_T - [AC]_T \times \frac{(\theta_{TKS} - \theta_{obs})}{\theta_{TKS}} \quad (13)$$

Job Plots. Solutions of AC and solutions of TKS159 were prepared at concentrations of 0.8, 0.6, 0.5, 0.4, and 0.2 mM. Solutions were mixed to make a solution with a total concentration of AC + TKS159 of 1.0 mM. CD spectra of all solutions were measured at 25 and 0 °C, and the CD spectral changes at 389 nm were plotted against [AC]/([AC] + [TKS159]).

DFT Calculations. All calculations were performed on Linux-PCs using the TURBOMOLE 5.9 program suite.[64] The resolution of identity (RI) approximation[65−69] was employed in all geometry optimizations, and the corresponding auxiliary basis sets were taken from the TURBOMOLE basis set library.

(62) Bohne, C.; Redmond, R. W.; Scaiano, J. C. In *Photochemistry in Organized & Constrained Media*; Ramamurthy, V., Ed.; VCH Publishers, Inc.: New York, 1991; pp 79−132.
(63) Nishijima, M.; Wada, T.; Nagamori, K.; Inoue, Y. *Chem. Lett.* **2009**, *38*, 726–727.
(64) Ahlrichs, R. et al. *TURBOMOLE*, version 5.9 Universität Karlsruhe, Karlsruhe. See also: http://www.cosmologic.de/QuantumChemistry/main_turbomole.html, 2005.
(65) Eichkorn, K.; Treutler, O.; Öhm, H.; Häser, M.; Ahlrichs, R. *Chem. Phys. Lett.* **1995**, *240*, 283–289.
(66) Grimme, S.; Waletzke, M. *Phys. Chem. Chem. Phys.* **2000**, *2*, 2075–2081.
(67) Hättig, C.; Weigend, F. *J. Chem. Phys.* **2000**, *113*, 5154–5161.
(68) Vahtras, O.; Almlöf, J.; Feyereisen, M. *Chem. Phys. Lett.* **1993**, *213*, 514–518.
(69) Weigend, F.; Häser, M. *Theor. Chem. Acc.* **1997**, *97*, 331–340.

Diastereomeric AC−TKS and AC−TM complexes were fully optimized at the dispersion corrected DFT-D/B-LYP level without symmetry constraints (C_1 symmetry) using an AO basis set of valence triple-ζ quality with a set of polarization functions (TZVP) with numerical quadrature multiple grid (m4 in TURBOMOLE terminology). The subsequent single-point energy calculations of the optimized structures were performed by using the SCS-MP2 method with the basis-set of TZVPP,[70−75] and the result was used for the calculation of the final Boltzmann distribution among the conformers.[76−78]

Acknowledgment. Y.I. and T.M. thank the Japan Science and Technology Agency and the Japan Society for the Promotion of Science for the support of the research carried out at Osaka University; Y.I. and T.C.S.P. thank the Global COE Program on Bio-Environmental Chemistry, Osaka University, for the support of the stay of T.C.S.P. at Osaka University; T.M. thanks the Mitsubishi Chemical Corporation Fund and Y.K. thanks the Uomoto International Scholarship Foundation for the support of their stay at UVic. T.C.S.P. and C.B. thank Natural Sciences and Engineering Research Council of Canada (NSERC) for support of the research carried out at the University of Victoria, and T.C.S.P. thanks NSERC for a CGS-D scholarship.

(70) Gerenkamp, M.; Grimme, S. *Chem. Phys. Lett*. **2004**, *392*, 229–235.
(71) Goumans, T. P.; Ehlers, A. W.; Lammertsma, K.; Wülthwein, E.-U.; Grimme, S. *Chem. Eur. J*. **2004**, *10*, 6468–6475.
(72) Grimme, S. *J. Chem. Phys*. **2003**, *118*, 9095–9102.
(73) Grimme, S. *J. Comput. Chem*. **2003**, *24*, 1529–1537.
(74) Grimme, S. *J. Phys. Chem. A* **2005**, *109*, 3067–3077.
(75) Piacenza, M.; Grimme, S. *J. Comput. Chem*. **2004**, *25*, 83–99.
(76) Mori, T.; Grimme, S.; Inoue, Y. *J. Org. Chem*. **2007**, *72*, 6998–7010.
(77) Mori, T.; Inoue, Y.; Grimme, S. *J. Phys. Chem. A* **2007**, *111*, 4222–4234.
(78) Mori, T.; Inoue, Y.; Grimme, S. *J. Phys. Chem. A* **2007**, *111*, 7995–8006.

Supporting Information Available: UV−vis, fluorescence and circular dichroism spectra of AC complexed to TKS159 or TM166 (Figures S1−S8), time-resolved fluorescence decays for AC−TKS (Figure S9), lifetimes for AC complexed to TKS159 or TM166 at different AC/template ratios and temperatures (Tables S1−S5), product studies for AC−TKS (Table S6), NMR for ACOMe (Figure S10), table (S7) with the atomic coordinates for the DFT-D-calculated AC−TKS or AC−TM complexes, and the complete ref 64. This material is available free of charge via the Internet at http://pubs.acs.org.